



C–P bond forming reactivity of N-heteropentacene: Isolation and characterization of a phospho-ylide complex of ruthenium(II)

Pradip Ghosh^a, Subhas Samanta^a, Alfonso Castiñeiras^b, Sreebrata Goswami^{a,*}

^a Department of Inorganic Chemistry, Indian Association for the Cultivation of Science, Jadavpur, Kolkata 700 032, India

^b Departamento de Química Inorgánica, Universidade de Santiago de Compostela, Campus Universitario Sur, 15782 Santiago de Compostela, Spain

ARTICLE INFO

Article history:

Received 30 January 2010

Received in revised form 12 March 2010

Accepted 16 March 2010

Available online 27 March 2010

Dedicated to Prof. Animesh Chakravorty

Keywords:

Ruthenium complex
C–P bond formation
C–O bond formation
Phospho-ylide complex
X-ray structure
Redox

ABSTRACT

In an unusual reaction of H_2L^2 ($H_2L^2 = N$ -heteropentacene) with $Ru(PPh_3)_3Cl_2$ a phospho-ylide ruthenium(II) complex (**1**) was obtained via unprecedented chemical transformations of the conjugate base $[L^2]^{2-}$. A bidentated phospho-ylide ligand is formed with concomitant aromatic ring hydroxylation and new C–P bond formation reactions. The new ligand, binds to Ru^{II} as a neutral N, O-donor. Crystal structure determination by single crystal X-ray diffraction has been used to characterize the compound. The phospho-ylide $Ru(II)$ description of the complex was established based on ^{13}C as well as ^{31}P NMR studies. The complex shows rich spectral and redox properties. UV–Vis–NIR spectrum consisted of multiple low-energy transitions in the visible and near IR regions. Preliminary density functional theory calculations were employed to understand the electronic structure and to assign the spectral transitions. Cyclic voltammogram and EPR-spectrum of the electrogenerated oxidized compound are reported and used to characterize the redox properties.

© 2010 Elsevier B.V. All rights reserved.

1. Introduction

Formation of carbon–heteroatom bonds [1–6] by transition metal as mediator has been the subject of intensive investigation in recent years because these allow syntheses [7–9] of novel molecules of acknowledged importance in pharmaceuticals and biology. Many of these compounds otherwise are difficult to synthesize or even inaccessible following the conventional synthetic protocols. In this respect majority of the efforts have been focused on the formation of carbon–nitrogen [10–18], –oxygen [19–22], and –sulfur bonds [23–26]. In comparison, however, carbon–phosphorus bond formation reactions are scanty in the literature [27–34]. It is relevant to note here that phosphorus containing molecules are versatile reagents in organic syntheses [35] and are useful hemilabile ligands [36–38]. Hemilabile phosphorous containing ligands are advantageous for their use in homogeneous metal catalyzed organic transformations since these can mask coordination site(s) effectively and liberate during the course of chemical transformations.

We have long standing interest in the metal-promoted oxidative carbon–nitrogen bond formation reactions of aromatic amines using transition metal as the mediator [39–52]. For example, we have described an unusual polymerization reaction of *p*-anisidine to an *N*-substituted phenazine derivative (HL^1) using hydrated $FeCl_3$ as the mediator [48]. Several new and regioselective C–N

bond formation reactions are operative in the above transformation. Furthermore, it has been shown that HL^1 , upon deprotonation, acts as a bidentated ligand and undergoes fascinating chemical transformations [52] including oxygenation and dimerization reactions as depicted in Scheme 1.

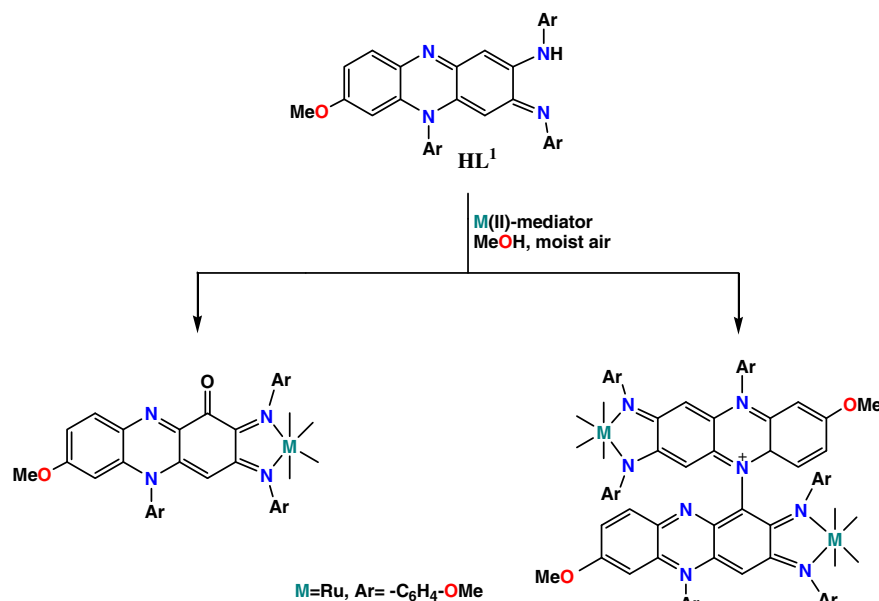
Encouraged by the above results, we became curious to study the coordination behaviour of polyheterocycles like phenazines. Literature survey has revealed that there has been extensive current literature on heteropentacene compounds because of their versatile π -functional material property [53] though their coordination behaviour remains unexplored. In this work, we present our results on the reaction of $Ru(PPh_3)_3Cl_2$ and *N*-heteropentacene (H_2L^2). An unprecedented chemical transformation occurred with the formation of a novel ruthenium complex (**1**) of a new phosphorous ylide ligand. Notably the chemistry of metal complexes with ylide is a subject of considerable current interest [54] in the context of their versatile coordinating behaviour. Successful isolation and complete characterization of the aforesaid complex constitute the primary concern of this work.

2. Results and discussion

2.1. Synthesis and characterization

The availability of the two nitrogen donor sites of the *N*-heteropentacene, H_2L^2 for alkylation [55] prompted us to explore its

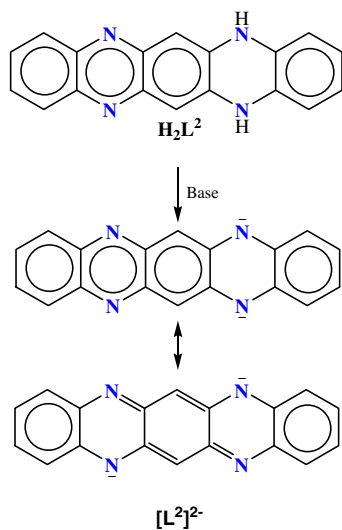
* Corresponding author. Tel.: +91 3324734971; fax: +91 3324732805.
E-mail address: icsg@iacs.res.in (S. Goswami).



Scheme 1.

coordination chemistry with transition metal ions. In alkaline conditions, the two N–H protons of H_2L^2 are known to undergo deprotonation and the corresponding conjugate base remains in equilibrium with its quinonoid form as shown in Scheme 2. In this work we have chosen $Ru(PPh_3)_3Cl_2$ as the starting complex to explore its coordination chemistry. Facile substitution reactions in the starting Ru-complex have been well documented in the literature. It may be relevant to add here that Ru^{II} and Os^{II} complexes of planar nitrogen containing ligands like phenazine can intercalate [56,57] DNA and RNA effectively and represent an important class of molecular probes.

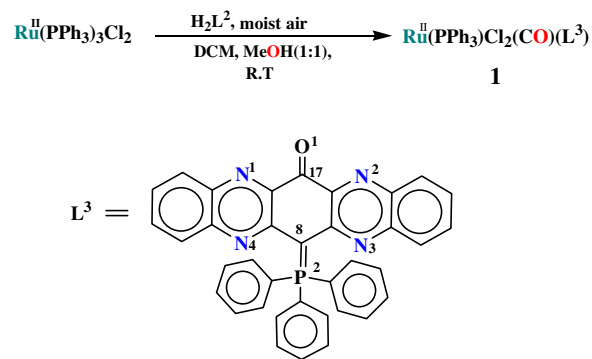
The compound H_2L^2 reacts smoothly with $Ru(PPh_3)_3Cl_2$ in methanol–dichloromethane solvent mixture at 300 K yielding a mixture of many products. TLC-purification of the mixture gave a crystalline yellowish-brown compound **1** as one of the products. The chemical reaction is shown in Scheme 3. The formation of the compound **1** is associated with an unexpected chemical transformation that occurred at the coordinated H_2L^2 . A bidentate



Scheme 2.

phospho-ylide ligand (L^3) is formed from the N-heteropentacene *via* (i) concomitant hydroxylation at C17 and (ii) a new C–P bond formation at the C8 site (Scheme 3). The new ligand, thus formed, binds to Ru^{II} as a neutral N, O-donor. The most striking part of the reference chemical transformation is the formation of a new C–P bond, which occurs *via* the migration of PPh_3 from ruthenium to C8 carbon to form a phospho-ylide ligand. The reaction occurs in moist air as it happens in the metal mediated hydroxylation of coordinated phenazines. Identical reaction sequences involving oxidation of the metal centre followed by hydroxylation of the polarized heteropentacene ring are operative in this transformation. The source of CO in this reaction is presumably methanol, since the chemical transformations did not occur in methanol-free solvent. The mixed ligand complex **1** was obtained in 20% yield. The poor yield of the compound is consistent with its slow decomposition in solution to a mixture of unidentified products even at a room temperature. Notably, the phospho-ylide part in the molecule is free which accounts for the instability/high reactivity of the molecule. We are yet to obtain any other pure products from the above chemical reaction due to serious overlap of bands on the TLC plate.

The complex **1** gave satisfactory elemental analysis (*cf.*, Section 4). Electrospray mass spectrum of the complex corroborate with its formulation as shown in Scheme 3. For example, it showed an in-



Scheme 3.

tense peak due to the molecular ion $[1-\text{Cl}]^+$ at m/z 985 amu. Notably, the experimental spectral feature of the Ru-complex corresponds very well to the simulated isotopic pattern for the given formulation (Fig. 1). The ^1H NMR spectrum of the compound, $[\text{Ru}(\text{PPh}_3)(\text{CO})\text{Cl}_2\text{L}^2]$ contains several overlapping resonances in the aromatic region, owing to the presence of a large number of unique protons in the complex. However, ^{13}C and ^{31}P NMR spectra of the complex are useful for its characterization. ^{31}P and ^{13}C NMR signals at 15.08 and 69.16 ppm, respectively confirm the existence of the ylidic $\text{P}=\text{C}$ bond [54] in the molecule. ^{13}C resonance due to the quaternary carbons of $\text{C}\equiv\text{O}$, and keto-carbonyl carbon, were also observed at 212 and 182 ppm, respectively. The additional peak in the ^{31}P NMR spectrum due to the Ru-coordinated PPh_3 was observed at 49.09 ppm. Segmented ^{13}C and ^{31}P NMR spectra are displayed in Fig. 2. Full range spectra (^1H , ^{13}C) are submitted as Supplementary material (Fig. S1). In the IR spectrum of the complex, two characteristic stretching frequencies for the terminal CO and keto-carbonyl function ($>\text{C}=\text{O}$) appeared at 1935 and 1740 cm^{-1} , respectively.

2.2. Crystal structure

Suitable crystals for X-ray structure determination of **1** were obtained by slow diffusion of a dichloromethane solution of the compound into hexane. Structural analysis of it indeed confirmed a novel Ru-mediated chemical transformation of the reference heteropentacene molecule. Its molecular view is shown in Fig. 3. ORTEP presentation and packing diagrams are submitted as Supplementary Figs. S2 and S3, respectively. The selected bond lengths and bond angles are collected in Table 1. The molecule **1** is hexa-coordinated and the coordination sphere has a distorted octahedral geometry. Moreover, the bond between Ru and the metal-coordinating atoms of the ylide ligand *viz.* Ru–N1 (2.185(4) Å)

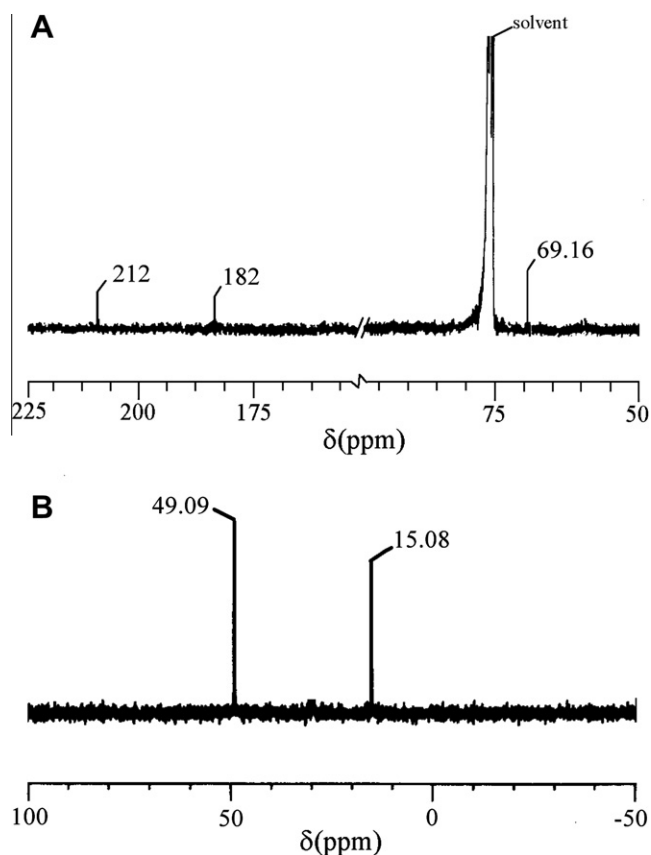


Fig. 2. Segmented NMR spectra of the complex **1** in CDCl_3 : (A) ^{13}C and (B) ^{31}P .

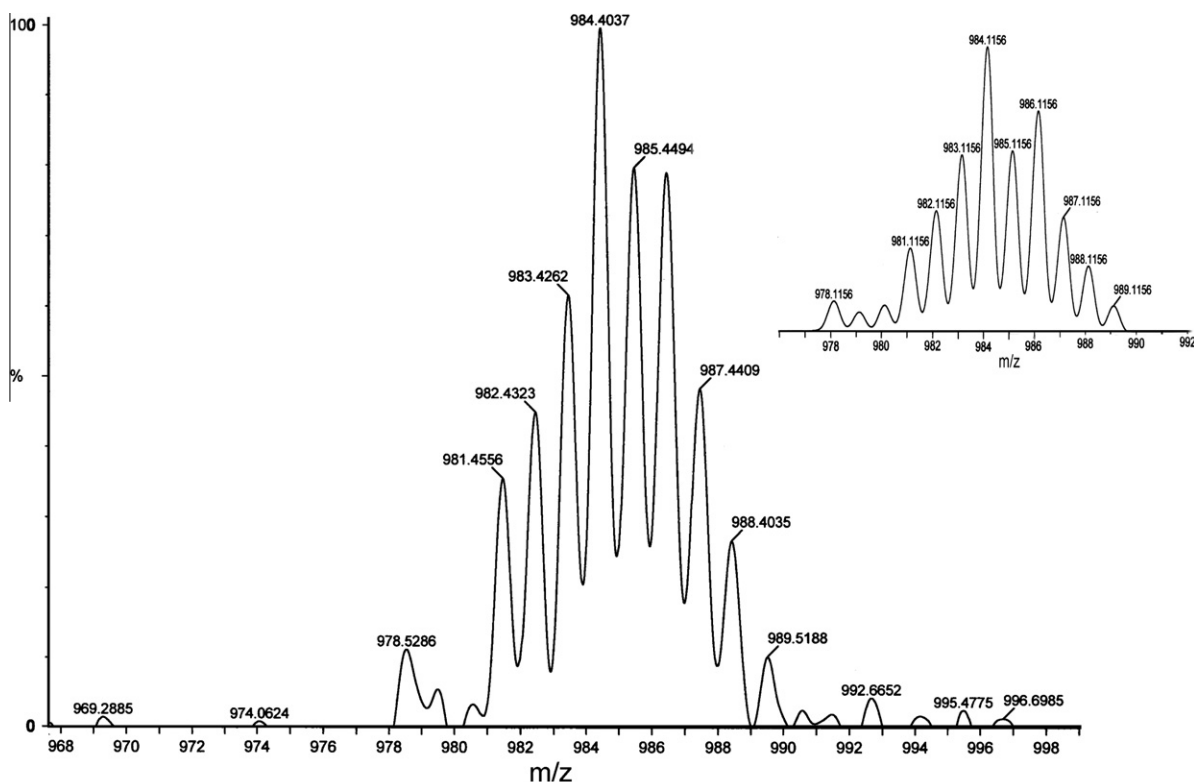


Fig. 1. ESI-MS spectrum of the complex **1** in CH_3CN ; simulated spectrum is shown as an inset.

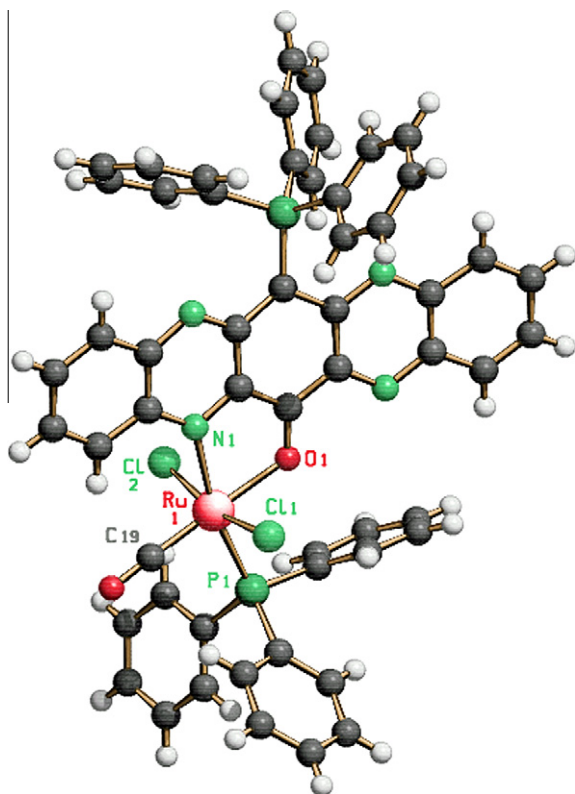


Fig. 3. Molecular view of the complex **1**.

Table 1
Selected experimental and calculated bond lengths (Å) of **1**.

Bonds	Experimental	Calculated
Ru1–O1	2.111(4)	2.130
Ru1–N1	2.185(4)	2.210
N1–C1	1.352(6)	1.371
C1–C2	1.413(6)	1.422
C2–C3	1.349(8)	1.377
C3–C4	1.419(8)	1.425
C4–C5	1.344(7)	1.377
C5–C6	1.418(7)	1.424
C6–N4	1.338(6)	1.357
N4–C7	1.338(6)	1.349
C7–C8	1.436(7)	1.435
C8–C9	1.428(7)	1.430
C9–N3	1.353(6)	1.357
N3–C10	1.341(7)	1.359
C10–C11	1.420(7)	1.424
C11–C12	1.356(9)	1.379
C12–C13	1.400(9)	1.428
C13–C14	1.346(9)	1.378
C14–C15	1.418(9)	1.423
C15–N2	1.352(6)	1.361
N2–C16	1.338(7)	1.337
C16–C17	1.447(7)	1.455
C17–O1	1.256(6)	1.275
C8–P2	1.769(5)	1.777

and Ru–O1 (2.111(4) Å) are similar to those observed in a related complex of an oxo-phenazine ligand [58]. The bond length C17–O1 (1.256(6) Å) indicates a localized double bond and the ligand coordinates as a neutral N,O- donor, which implies the bivalent oxidation state of the central ruthenium metal. Interestingly, the two C–C bonds around the C8 carbon, *viz.* C7–C8 (1.436(7) Å) and

C8–C9 (1.428(7) Å) are single bonds, while the C8–P2 bond (1.769(6) Å) is close to an ideal ylidic C=P bond length [54,59] (Scheme 3 and Table 1). The two possible resonating forms [54] of the complex are shown in Scheme 4.

2.3. Cyclic voltammetry and EPR

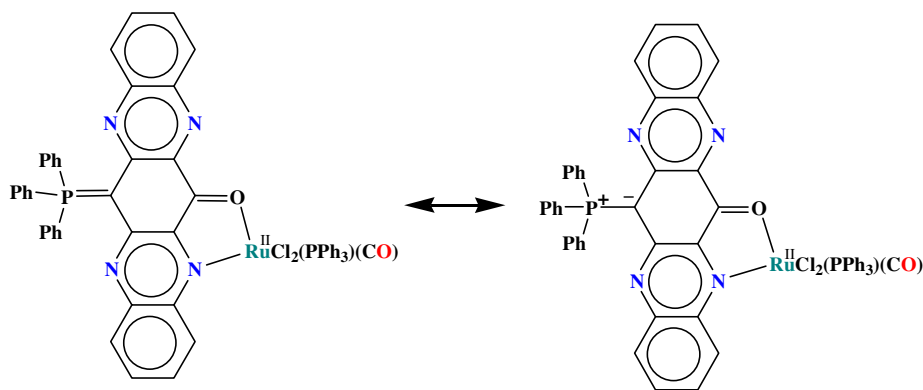
The redox behaviour of the complex **1** was studied by cyclic voltammetry in dichloromethane (0.1 M TBAP) in the potential range between +1.8 and –1.8 V and using a platinum disc as working electrode. The potentials are referenced to the saturated Ag/AgCl electrode. It shows two waves in the above potential range (Fig. 4). A reversible oxidative response appeared near 0.42 V; the second response is irreversible and occurs at a cathodic potential, –1.0 V. One-electron stoichiometry of the reversible anodic wave was confirmed by exhaustive electrolysis of **1** at 0.6 V. Oxidation occurs at the metal centre while the redox process occurring at the cathodic potential is due to the ligand reduction. These results are corroborated by density functional theory (DFT) calculations, which show that the HOMO and LUMO of the complex are primarily metal and ligand centred, respectively (see below). One-electron oxidized complex **1**⁺ showed a rhombic EPR-spectrum (Fig. 5) with characteristic splitting pattern of the *g* components in frozen solution (*cf.* Section 4). Two close lying components *g*₁, *g*₂ > 2 are complemented by *g*₃ < 2. Taken together *g*_{av} is >2 – a typical [60] for a low-spin d⁵ situation (Ru^{III}) with not-too-distorted octahedral ligation. Thus the EPR-spectrum of the electro-generated compound implies that the oxidation of **1** primarily occurs at the ruthenium(II) centre.

2.4. UV–Vis spectra and DFT

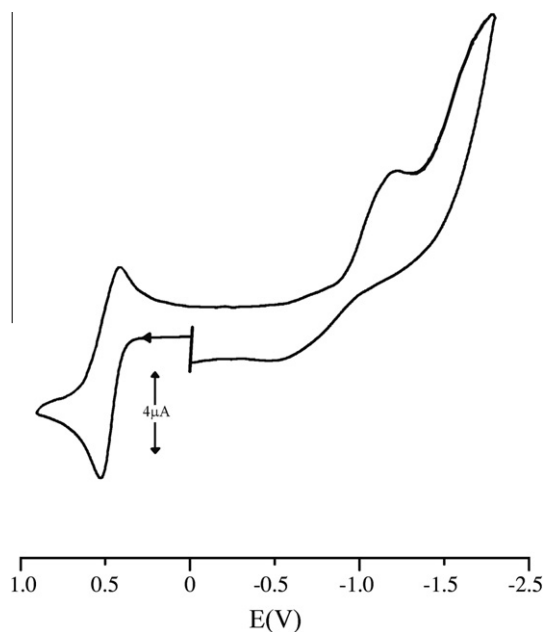
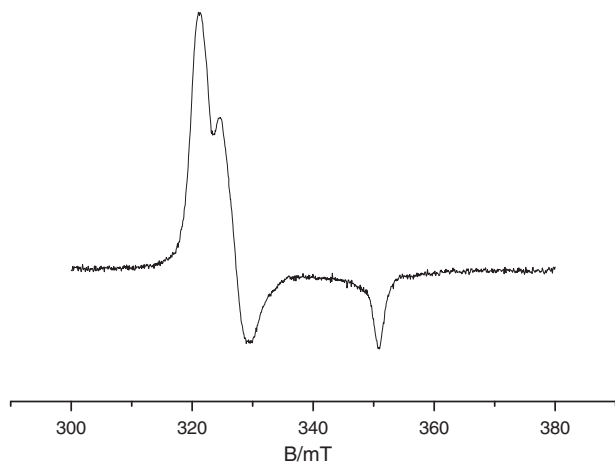
The compound exhibits several low-energy absorptions in the UV–Vis and near IR region of the spectrum with two broad bands at 730 and 875 nm (Table 2, Fig. 6). The assignment of these bands is guided by the results of Density Functional Theory (DFT) calculations. Before calculation of the excitation energies using time-dependent DFT (TD-DFT) formalism, the molecular structure of **1** was fully optimized at the B3LYP level of theory. The calculated bond lengths and angles can be compared well to the crystallographically established metrical parameters (Table 1). Overall there is a good agreement with the two sets of numbers as bond lengths and angles are predicted within 2 pm and 1°–4° from the experimental values, respectively.

The calculated excitation energies for **1** are collected in Table 3. The two peaks with transition maxima at 875 and 730 nm can be readily assigned to ¹A (HOMO–1 → LUMO) and ¹A (HOMO–2 → LUMO). These transitions are computationally predicted at 880 and 679 nm, respectively. Several possible transitions were found to lie between 300 and 600 nm. However, calculated oscillator strengths predict that transitions at 875, 730, 460, 405 and 330 nm should dominate the spectrum. Calculated spectrum is shown in Supplementary Fig. S4 for comparison. The highest oscillator strength is calculated for the ¹A transition (predominately HOMO → LUMO+2 transition) at 305 nm which is in excellent agreement with the experimentally observed band maximum at 330 nm.

An analysis of the MOs of the complex reveals that the highest occupied orbitals, HOMO and HOMO–1 are centred on ruthenium while the HOMO–2 is substantially localised (Fig. 7) on the carbon bonded to PPh₃ of the ylide ligand (**L**³). The lowest unoccupied MOs, LUMO, LUMO+1 and LUMO+2 are primarily localised on the ylide ligand. Thus the charge-transfer transition appearing at 875 nm is of MLCT type and the transition at 730 nm may best be described as an intra-ligand charge-transfer (ILCT) transition.



Scheme 4.

Fig. 4. Cyclic voltammogram of the complex **1** in CH_2Cl_2 .Fig. 5. EPR-spectrum of the complex **1**.

3. Conclusion

In an unusual chemical reaction of the N-heteropentacene compound H_2L^2 and $\text{Ru}(\text{PPh}_3)_3\text{Cl}_2$, a ruthenium(II) complex of phos-

pho-ylide ligand was isolated. X-ray structure determination of the complex has confirmed the formation of a Ru^{II} -ylide complex via a series of unprecedented chemical transformations including hydroxylation as well as C–P bond formation at heteropentacene ring. The ruthenium complex showed several low-energy transitions in the visible and near IR region of the spectrum. These are assigned to metal-to-ligand and intra-ligand charge-transfer transitions. Preliminary density functional theory calculations were employed to overview the electronic structure, redox and spectroscopic assignments.

4. Experimental

4.1. Materials

The starting metal complex $\text{Ru}(\text{PPh}_3)_3\text{Cl}_2$ was synthesized according to the literature procedure [61]. 1,2-diaminobenzene was purchased from Loba chemicals, (India). 2,5-Dihydroxy *p*-benzoquinone was an Aldrich reagent and the solvents used were obtained from Qualigens and MERCK (India). The ligands were synthesized [53] following the literature procedure. Tetrabutylammonium perchlorate (TBAP) was prepared and recrystallized as reported before [62]. All other chemicals were of reagent grade and used as received. *Caution!* perchlorate salts have to be handled with care and with appropriate safety precautions.

4.2. Methods

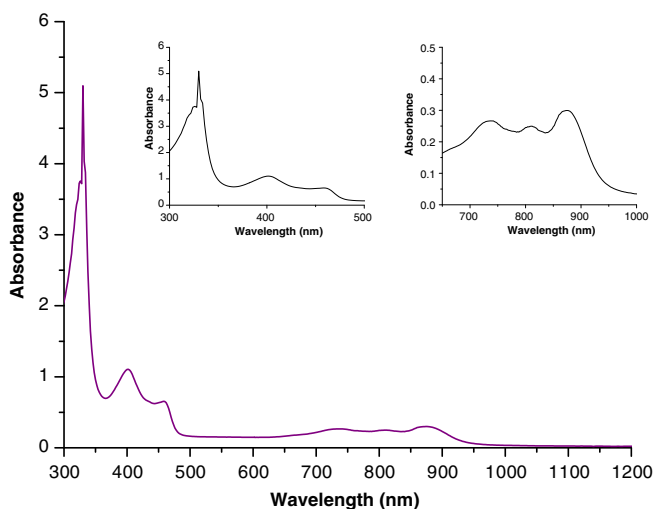
UV–Vis–NIR absorption spectrum was recorded on a Perkin–Elmer Lambda 950 UV/Vis spectrophotometer. NMR spectra were taken on a Bruker Avance DPX 300 spectrometer. Infrared spectra were obtained using a Perkin–Elmer 783 spectrophotometer. Cyclic voltammetry was carried out in 0.1 M Bu_4NClO_4 solutions using a three-electrode configuration (platinum disc working electrode, Pt counter electrode, Ag/AgCl reference electrode) and a PC-controlled PAR model 273A electrochemistry system. The $E_{1/2}$ for the ferrocenium–ferrocene couple under our experimental condition was 0.39 V. A Perkin–Elmer 240C elemental analyzer was used to collect micro analytical data (C, H, N). ESI mass spectrum was recorded on a micro mass Q-TOF mass spectrometer (serial no. YA 263). EPR-spectrum in the X band was recorded with a JEOL JES-FA200 spectrometer.

4.3. Synthesis

A mixture of 100 mg (0.10 mmol) of $\text{Ru}(\text{PPh}_3)_3\text{Cl}_2$ and 30 mg (0.106 mmol) of the ligand H_2L^2 was stirred for 36 h in 1:1 dichloromethane-methanol solvent mixture. The initial bluish color

Table 2
Experimental and TD-DFT calculated transitions of the complex **1**.

Symmetry	Excitation energy (10^3 cm^{-1})	oscillator strength	Dominant contributions (>5%)	Experimentally observed transitions in nm ($\epsilon, \text{ mol}^{-1}\text{cm}^{-1}$)
¹ A	11.024 (907) ^a	0.0533	HOMO → LUMO (10%) HOMO-1 → LUMO (74%)	875 (2939)
¹ A	14.618 (684)	0.0371	HOMO-2 → LUMO (82%)	730 (2600)
¹ A	19.858 (503)	0.0321	HOMO-1 → LUMO+1 (92%)	
¹ A	22.678 (440)	0.0355	HOMO-6 → LUMO (34%) HOMO-2 → LUMO+1 (49%)	460 ^b
¹ A	25.277 (395)	0.0211	HOMO-11 → LUMO (38%) HOMO-9 → LUMO (20%) HOMO-1 → LUMO+5 (11%) HOMO-10 → LUMO (7%) HOMO-8 → LUMO (5%)	
¹ A	26.417 (378)	0.036	HOMO-11 → LUMO (74%) HOMO-10 → LUMO (64%)	
¹ A	28.001 (357)	0.0444	HOMO-12 → LUMO (48%) HOMO-2 → LUMO+2 (10%) HOMO-1 → LUMO+2 (26%)	
¹ A	28.990 (344)	0.1068	HOMO-13 → LUMO (22%) HOMO-2 → LUMO+2 (14%) HOMO-1 → LUMO+2 (50%)	405 (11 100)
¹ A	31.840 (314)	0.0599	HOMO-6 → LUMO+1 (68%) HOMO-1 → LUMO+3 (18%)	
¹ A	32.849 (304)	0.8712	HOMO-2 → LUMO+2 (48%) HOMO-13 → LUMO (7%) HOMO-1 → LUMO (74%)	330 (50 600)

^a Values in parentheses are in nm.^b Broad shoulder.**Fig. 6.** UV-Vis-NIR spectrum of the complex **1**. Segmented spectra are shown as insets using different absorbance scale.

changed to brown. The mixture was evaporated on a rotary evaporator. The crude mass, thus obtained, was loaded on a preparative silica TLC plate for purification using dichloromethane as the eluent. A yellowish-brown band of the complex, **1** was collected and crystallized from CH_2Cl_2 - C_6H_{14} solvent mixture. Several overlapping bands of different colors follow the above brown band. We are yet to isolate any other pure product from the above TLC-purification. The characterization data of the complex are as follows: Yield: 20%. ESI-MS (in acetonitrile solvent): 985 m/z $[\text{M}-\text{Cl}]^+$. IR (in KBr disk): 1935 $\nu_{(\text{C}=\text{O})}$, 1740 $\nu_{(\text{C}=\text{O})}$, 1585 $\nu_{(\text{C}=\text{N})}$, EPR $[\text{1}]^+$ (in dichloromethane glass at 77 K): 2.139(g1) 2.116(g2) 1.946(g3). CV (in dichloromethane at 298 K with TBAP as supporting

Table 3
Crystallographic data of **1**.

	1
Empirical formula	$\text{C}_{55}\text{H}_{38}\text{Cl}_2\text{N}_4\text{O}_2\text{P}_2\text{Ru}$
Molecular mass	1020.80
<i>T</i> (K)	296
Crystal system	monoclinic
Space group	$P2_1/n$
<i>a</i> (Å)	11.6531(5)
<i>b</i> (Å)	31.3838(14)
<i>c</i> (Å)	12.6550(6)
α (°)	90
β (°)	98.447(1)
γ (°)	90
<i>V</i> (Å ³)	4578.0(4)
<i>Z</i>	4
<i>D</i> _{calcd} (g cm ⁻³)	1.481
Crystal dimensions (mm)	$0.15 \times 0.17 \times 0.22$
θ Range for data collection (°)	1.3–27.5
Goodness-of-fit (GOF)	1.03
Reflections collected	10 464
Largest difference between peak and hole ($e \text{ \AA}^{-3}$)	1.38, -1.29
Final <i>R</i> indices [<i>I</i> > 2 σ (<i>I</i>)]	0.0346, 0.0762

electrolyte): 0.42 V (reversible), -1.0 V (irreversible). *Anal. Calc.* for $\text{C}_{55}\text{H}_{38}\text{Cl}_2\text{N}_4\text{O}_2\text{P}_2\text{Ru}$: C, 64.78; H, 3.82; N, 5.54 Found: C, 64.75; H, 3.79; N, 5.51%.

4.4. Crystallographic measurement

Crystallographic data of the compound **1** are collected in Table 3. Suitable X-ray quality crystals of it were obtained as noted before.

All data were collected on a Bruker SMART APEX-II diffractometer, equipped with graphite monochromatic Mo $K\alpha$ radiation

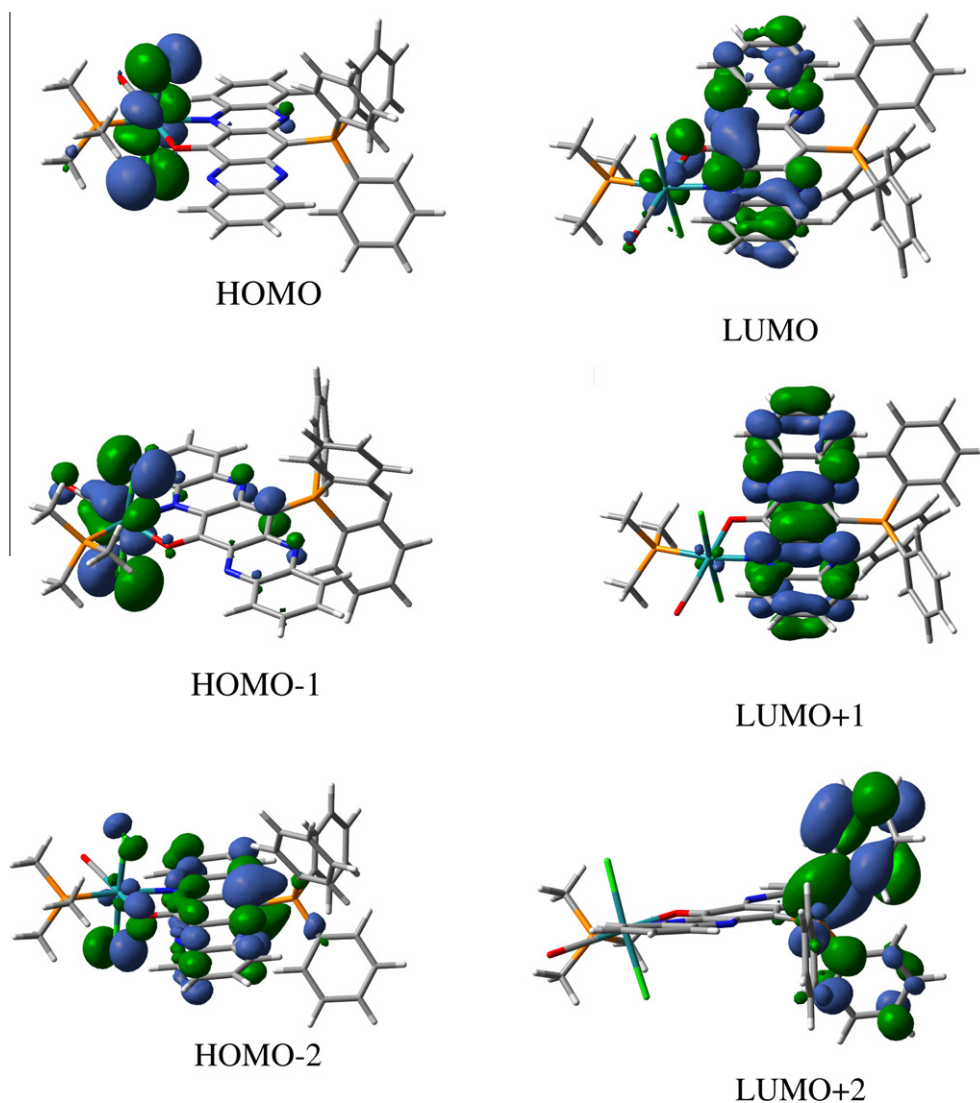


Fig. 7. Frontier molecular orbitals of the complex **1** in 0.03 isosurface value.

($\lambda = 0.71073 \text{ \AA}$), and were corrected for Lorentz-polarization effects. The structure was solved by employing the SHELXS-97 program package [63] and refined by full-matrix least-squares based on F^2 (SHELXL-97) [64]. All hydrogen atoms were added in calculated positions.

4.5. Computational details

Full geometry optimization was carried out using the density functional theory method at the (R) B3LYP [65]. Calculations were performed without any symmetry constraints. H, C and N were assigned the 6-31G(d) basis set. P and Cl were assigned as 6-31G(d,p) basis set. The LanL2DZ basis set with effective core potential were employed for the ruthenium atom [66]. The Ru-coordinated triphenylphosphine (PPh_3) was replaced by trimethylphosphine (PMe_3). The vibration frequency calculation was performed to ensure that the optimized geometries represent the local minima and there are only positive Eigen values. All calculations were performed with the GAUSSIAN03 programme package [67]. Vertical electronic excitation based on B3LYP optimized geometries were computed using the time-dependent density functional theory (TD-DFT) formalism [68–70] in dichloromethane using conductor

like polarisable continuum model [71–73]. GAUSSSUM [74] was used to calculate the fractional contributions of various molecular orbital in the optical spectral transition.

Acknowledgements

Financial support received from the Council of Scientific and Industrial Research (CSIR), New Delhi (Project 01/2358/09/EMR-II) is gratefully acknowledged. Crystallography was performed at the DST-funded National Single Crystal Diffractometer Facility at the Department of Inorganic Chemistry, IACS. We are thankful to Dr. C.R. Sinha, Jadavpur University for his support in DFT calculation. P.G. and S.S. are thankful to the Council of Scientific and Industrial Research, New Delhi for fellowship support.

Appendix A. Supplementary material

CCDC 763983 contains the supplementary crystallographic data for this paper. These data can be obtained free of charge from The Cambridge Crystallographic Data Centre via www.ccdc.cam.ac.uk/data_request/cif. Supplementary data associated with this article

can be found, in the online version, at [doi:10.1016/j.ica.2010.03.043](https://doi.org/10.1016/j.ica.2010.03.043).

References

- [1] K. Godula, D. Sames, *Science* 312 (2006) 67.
- [2] J.B. Fulton, A.W. Holland, D.J. Fox, R.G. Bergman, *Acc. Chem. Res.* 35 (2002) 44.
- [3] K. Muñiz, *Chem. Soc. Rev.* 33 (2004) 166.
- [4] N. Hazari, P. Mountford, *Acc. Chem. Res.* 38 (2005) 839.
- [5] T.E. Müller, K.C. Hultzs, M. Yus, F. Foubelo, *Chem. Rev.* 108 (2008) 3795.
- [6] D.M. Roundhill, *Chem. Rev.* 92 (1992) 1.
- [7] R. Hili, A.K. Yudin, *Nat. Chem. Biol.* 2 (2006) 284.
- [8] A. Ricci (Ed.), *Amino Group Chemistry, From Syntheses to the Life Science*, Wiley-VCH, Weinheim, 2007.
- [9] J. Hassan, M. Sévignon, C. Gozzi, E. Schulz, M. Lemaire, *Chem. Rev.* 102 (2002) 1359.
- [10] S.H. Cho, J.Y. Kim, S.Y. Lee, S. Chang, *Angew. Chem., Int. Ed.* 48 (2009) 9127.
- [11] J.L. Brice, J.E. Harang, V.I. Timokhin, N.R. Anasthisi, S.S. Stahl, *J. Am. Chem. Soc.* 127 (2005) 2868.
- [12] J.D. Soper, W. Kaminsky, J.M. Mayer, *J. Am. Chem. Soc.* 123 (2001) 5594.
- [13] G. Bai, D.W. Stephan, *Angew. Chem., Int. Ed.* 46 (2007) 1856.
- [14] J.P. Wolfe, S. Wagaw, J.-F. Marcoux, S.L. Buchwald, *Acc. Chem. Res.* 31 (1998) 805.
- [15] A.R. Muci, S.L. Buchwald, *Top. Curr. Chem.* 219 (2002) 131.
- [16] D.S. Surry, S.L. Buchwald, *Angew. Chem., Int. Ed.* 47 (2008) 6338.
- [17] J.F. Hartwig, *Angew. Chem., Int. Ed.* 37 (1998) 2046.
- [18] J.F. Hartwig, *Acc. Chem. Res.* 41 (2008) 1534.
- [19] E.M. Beccalli, G. Broggini, M. Martinelli, S. Sottocornola, *Chem. Rev.* 107 (2007) 5318.
- [20] Y. Peng, L. Cui, G. Zhang, L. Zhang, *J. Am. Chem. Soc.* 131 (2009) 5062.
- [21] S. Protti, M. Fagnoni, A. Albini, *J. Am. Chem. Soc.* 128 (2006) 10670.
- [22] Jiajia Niu, Hua Zhou, Zhigang Li, Jingwei Xu, Shaojing Hu, *J. Org. Chem.* 74 (2009) 950.
- [23] T. Kondo, T. Mitsudo, *Chem. Rev.* 100 (2000) 3205.
- [24] K. Matsumoto, H. Sugiyama, *Acc. Chem. Res.* 35 (2002) 915.
- [25] R.Y.C. Shin, L.Y. Goh, *Acc. Chem. Res.* 39 (2006) 301.
- [26] M. Arisawa, K. Fujimoto, S. Morinaka, M. Yamaguchi, *J. Am. Chem. Soc.* 127 (2005) 12226.
- [27] D.J. Brauer, M. Hingst, K.W. Kottsieper, C. Liek, T. Nickel, M. Tepper, O. Stelzer, W.S. Sheldrick, *J. Organomet. Chem.* 645 (2002) 14.
- [28] A. Stadler, C.O. Kappe, *Org. Lett.* 4 (2002) 3541.
- [29] H.-B. Kraatz, A. Pletsch, *Tetrahedron: Asymmetry* 11 (2000) 1617.
- [30] D.E. Bergbreiter, Y.-S. Liu, S. Furyk, B.L. Case, *Tetrahedron Lett.* 39 (1998) 8799.
- [31] P. Machnitzki, T. Nickel, O. Stelzer, C. Landgrafe, *Eur. J. Inorg. Chem.* (1998) 1029.
- [32] O. Herd, A. Hesbeler, M. Hingst, M. Trepper, O. Stelzer, *J. Organomet. Chem.* 522 (1996) 69.
- [33] D. Cai, J.F. Payack, D.R. Bender, D.L. Hughes, T.R. Verhoeven, P.J. Reider, *J. Org. Chem.* 59 (1994) 7180.
- [34] D. Gelman, L. Jiang, S.L. Buchwald, *Org. Lett.* 5 (2003) 2315.
- [35] For a review see: B.E. Maryanoff, A.B. Reitz, *Chem. Rev.* 89 (1989) 863.
- [36] H. Grützmaier, *Angew. Chem., Int. Ed.* 47 (2008) 1814.
- [37] P. Braunstein, *J. Organomet. Chem.* 689 (2004) 3953.
- [38] P. Braunstein, F. Naud, *Angew. Chem.* 113 (2001) 702. *Angew. Chem., Int. Ed.* 40 (2001) 680.
- [39] S. Samanta, S. Goswami, *J. Am. Chem. Soc.* 131 (2009) 924.
- [40] S. Samanta, L. Adak, R. Jana, G. Mostafa, H.M. Tuononen, B.C. Ranu, S. Goswami, *Inorg. Chem.* 47 (2008) 11062.
- [41] K.N. Mitra, S. Goswami, *Chem. Commun.* (1997) 49.
- [42] K.N. Mitra, P. Majumder, S.-M. Peng, A. Castiñeiras, S. Goswami, *Chem. Commun.* (1997) 1267.
- [43] K.N. Mitra, S.-M. Peng, S. Goswami, *Chem. Commun.* (1998) 1685.
- [44] P. Majumder, L.R. Falvello, M. Tomás, S. Goswami, *Chem. Eur. J.* 7 (2001) 5222.
- [45] C. Das, S. Goswami, *Comments Inorg. Chem.* 24 (2003) 137.
- [46] K.N. Mitra, S. Goswami, *Inorg. Chem.* 36 (1997) 1322.
- [47] K.N. Mitra, S. Choudhury, A. Castiñeiras, S. Goswami, *J. Chem. Soc., Dalton Trans.* (1998) 2901.
- [48] A.K. Ghosh, K.N. Mitra, G. Mostafa, S. Goswami, *Eur. J. Inorg. Chem.* (2000) 1961.
- [49] A. Saha, A.K. Ghosh, P. Majumdar, K.N. Mitra, S. Mondal, K.K. Rajak, L.R. Falvello, S. Goswami, *Organometallics* 18 (1999) 3772.
- [50] A.K. Ghosh, P. Majumdar, L.R. Falvello, G. Mostafa, S. Goswami, *Organometallics* 18 (1999) 5086.
- [51] C. Das, A. Saha, S.-M. Peng, G.-H. Lee, S. Goswami, *Inorg. Chem.* 42 (2003) 198.
- [52] P. Banerjee, G. Mostafa, A. Castiñeiras, S. Goswami, *Eur. J. Inorg. Chem.* (2007) 412.
- [53] U.H.F. Bunz, *Chem. Eur. J.* 15 (2009) 6780. and references therein.
- [54] L.R. Falvello, J.C. Ginés, J.J. Carbó, A. Lledós, R. Navarro, T. Soler, E.P. Urriolabeitia, *Inorg. Chem.* 45 (2006) 6803. and references therein.
- [55] Q. Tang, J. Liu, H.S. Chan, Q. Miao, *Chem. Eur. J.* 15 (2009) 3965.
- [56] A.E. Friedman, J.-C. Chambron, J.-P. Sauvage, N.J. Turro, J.K. Barton, *J. Am. Chem. Soc.* 112 (1990) 4960.
- [57] E. Rüba, J.R. Hart, J.K. Barton, *Inorg. Chem.* 43 (2004) 4570.
- [58] P. Banerjee, A.D. Jana, G. Mostafa, S. Goswami, *Eur. J. Inorg. Chem.* (2008) 44.
- [59] L.R. Falvello, S. Fernández, R. Navarro, E.P. Urriolabeitia, *Inorg. Chem.* 36 (1997) 1136.
- [60] J.A. Weil, J.R. Bolton, *Electron Paramagnetic Resonance*, second ed., Wiley Interscience, New York, 2007.
- [61] T.A. Stephenson, G. Wilkinson, *J. Inorg. Nucl. Chem.* (1996) 945.
- [62] S. Goswami, R.N. Mukherjee, A. Chakravorty, *Inorg. Chem.* 22 (1983) 2825.
- [63] G.M. Sheldrick, *Acta Crystallogr., Sect. A* 46 (1990) 467.
- [64] G.M. Sheldrick, *SHELXL 97. Program for the Refinement of Crystal Structures*, University of Göttingen, Göttingen, Germany, 1997.
- [65] C. Lee, W. Yang, R.G. Parr, *Phys. Rev. B* 37 (1988) 785.
- [66] D. Andrae, U. Haeussermann, M. Dolg, H. Stoll, H. Preuss, *Theor. Chim. Acta* 77 (1990) 123.
- [67] M.J. Frisch, G.W. Trucks, H.B. Schlegel, G.E. Scuseria, M.A. Robb, J.R. Cheeseman, J.A. Montgomery, Jr., T. Vreven, K.N. Kudin, J.C. Burant, J.M. Millam, S.S. Iyengar, J. Tomasi, V. Barone, B. Mennucci, M. Cossi, G. Scalmani, N. Rega, G.A. Petersson, H. Nakatsuji, M. Hada, M. Ehara, K. Toyota, R. Fukuda, J. Hasegawa, M. Ishida, T. Nakajima, Y. Honda, O. Kitao, H. Nakai, M. Klene, X. Li, J.E. Knox, H.P. Hratchian, J.B. Cross, V. Bakken, C. Adamo, J. Jaramillo, R. Gomperts, R.E. Stratmann, O. Yazyev, A.J. Austin, R. Cammi, C. Pomelli, J.W. Ochterski, P.Y. Ayala, K. Morokuma, G.A. Voth, P. Salvador, J.J. Dannenberg, V.G. Zakrzewski, S. Dapprich, A.D. Daniels, M.C. Strain, O. Farkas, D.K. Malick, A.D. Rabuck, K. Raghavachari, J.B. Foresman, J.V. Ortiz, Q. Cui, A.G. Baboul, S. Clifford, J. Cioslowski, B.B. Stefanov, G. Liu, A. Liashenko, P. Piskorz, I. Komaromi, R.L. Martin, D.J. Fox, T. Keith, M.A. Al-Laham, C.Y. Peng, A. Nanayakkara, M. Challacombe, P.M.W. Gill, B. Johnson, W. Chen, M.W. Wong, C. Gonzalez, J.A. Pople, Inc. Gaussian, CT, Wallingford, 2004.
- [68] R. Bauernschmitt, R. Ahlrichs, *Chem. Phys. Lett.* 256 (1996) 454.
- [69] R.E. Stratmann, G.E. Scuseria, M.J. Frisch, *J. Chem. Phys.* 109 (1998) 8218.
- [70] M.E. Casida, C. Jamorski, K.C. Casida, D.R. Salahub, *J. Chem. Phys.* 108 (1998) 4439.
- [71] V. Barone, M. Cossi, *J. Phys. Chem. A* 102 (1998) 1995.
- [72] M. Cossi, V. Barone, *J. Chem. Phys.* 115 (2001) 4708.
- [73] M. Cossi, N. Rega, G. Scalmani, V. Barone, *J. Comput. Chem.* 24 (2003) 669.
- [74] N.M. O'Boyle, A.L. Tenderholt, K.M. Langner, *J. Comput. Chem.* 29 (2008) 839.